Supporting Information

Modelling Atmospheric Mineral Aerosol Chemistry to Predict Heterogeneous Photooxidation of SO_2

Zechen Yu, Myoseon Jang, and Jiyeon Park
P.O.Box116450, Department of Environmental Engineering Sciences, Engineering School of Sustainable Infrastructure and Environment, University of Florida, Gainesville, FL, USA, 32611
Correspondence to: Myoseon Jang (mjang@ufl.edu)

Number of Tables: 1

Number of Figures: 8

Section 1: Chamber Characterization

The outdoor experiments were conducted using the University of Florida Atmospheric Photochemical Outdoor Reactor (UF–APHOR) dual chambers located on the roof of Black Hall at University of Florida, Gainesville, Florida (latitude/longitude: 29.64185°/-82.347883°). The total volume for the two half–cylinder shaped chamber is 52 m^3 each. The surface to volume ratio is 1.65 m^2 m^{-3} for each chamber. The chambers are built with 0.13 mm FEP Teflon film. The meteorological parameters (i.e., temperature, relative humidity, sunlight spectrum and sunlight intensity) are monitored simultaneously both inside and outside the chambers using a hygrometer (CR1000 Measurement and Control System, Campbell Scientific) (temperature and humidity), a fibro–optical portable spectrometer (EPP2000, Stellar Net Inc., USA) (sunlight spectrum) and an ultraviolet radiometer (TUVR, Eppley Laboratory Inc.) (sunlight intensity). In addition, the wall loss rate constants of ozone, SO_2, H_2O_2 and HONO were measured via separate experiments. The rate constant of particle loss to the chamber wall was also measured for Arizona Test Dust (ATD) particles as well as the ammonia sulfate inorganic seeded aerosol. The particle loss rate was calculated for every 3 minutes within each particle size bin and then integrated to calculate an average particle loss rate. The typical particle distribution of ATD particles is shown in the Fig. S1.

Indoor chamber experiment

The indoor chamber experiments were performed in a 2 m^3 Teflon indoor chamber equipped with UV lamps (Wavelength: 280nm – 900 nm) (Solarc Systems Inc., FS40T12/UVB). The RH and the concentration of trace gases and dust particles were controlled to variety specific experimental conditions. During the experiment, the gases were continuously measured directly from the indoor chamber using a gas chromatography–flam ionization detector (HP–5890 GC–FID), a fluorescence TRS analyzer (Teledyne Model 102E), and a chemiluminescence NO/NOx analyzer (Teledyne Model T201). The suspend particles were continuously measured by a scanning mobility particle sizer (SMPS, TSI 3080, USA) and an Optical Particle Counter (OPC, TSI 3330, USA). The mass concentration of inorganic iron was measured using a Particle–Into–Liquid Sampler (Applikon, ADISO 2081) combined with Ion Chromatography (Metrohm, 761 Compact IC) (PILS–IC) for every 30 minutes.

Outdoor chamber experiment

The dual chambers were flushed and cleaned by the air purifier system (GC Series, IQ Air Inc.) for 2 days before each experiment. The background sulfate concentration was measured every time

before experiments. Non–reactive CCL_4 (400 ppb) was injected into the dual chamber to determine the chamber dilution factor. Due to the chamber dilution, ambient trace gases (i.e., CO, O_3, CH_4, HCHO and volatile organic compounds) outside the chamber are intruded into the chamber. The estimated concentration of background gases are 1.8 ppb CH_4, 18 ppb HCHO, 6 ppb CH_3CHO, 0.1 ppb isoprene and 1 ppb HONO. The measurement procedures of gases and inorganic iron concentration were similar to that of indoor chamber experiments. The particle distribution was measured using the SMPS and the OPC. For measuring the total particle mass concentration, the suspended particles were collected on a 13mm diameter Teflon–coated glass fiber filter (Pall Life Science Pallflex, TX40HI20–WW) for 20 minutes. The filter mass difference was measured using a microbalance (MX5, Mettler Toledo, Columbus, OH). The temperature (T, K) and relative humidity (RH, %) in the dual chamber were monitored using a hygrometer (CR1000 Measurement and Control System, Campbell Scientific). For measuring the wavelength–dependent actinic flux, a fibro–optical portable spectrometer (EPP2000, Stellar Net Inc., USA) and an ultraviolet radiometer (TUVR, Eppley Laboratory Inc.) were used.

Figure S1

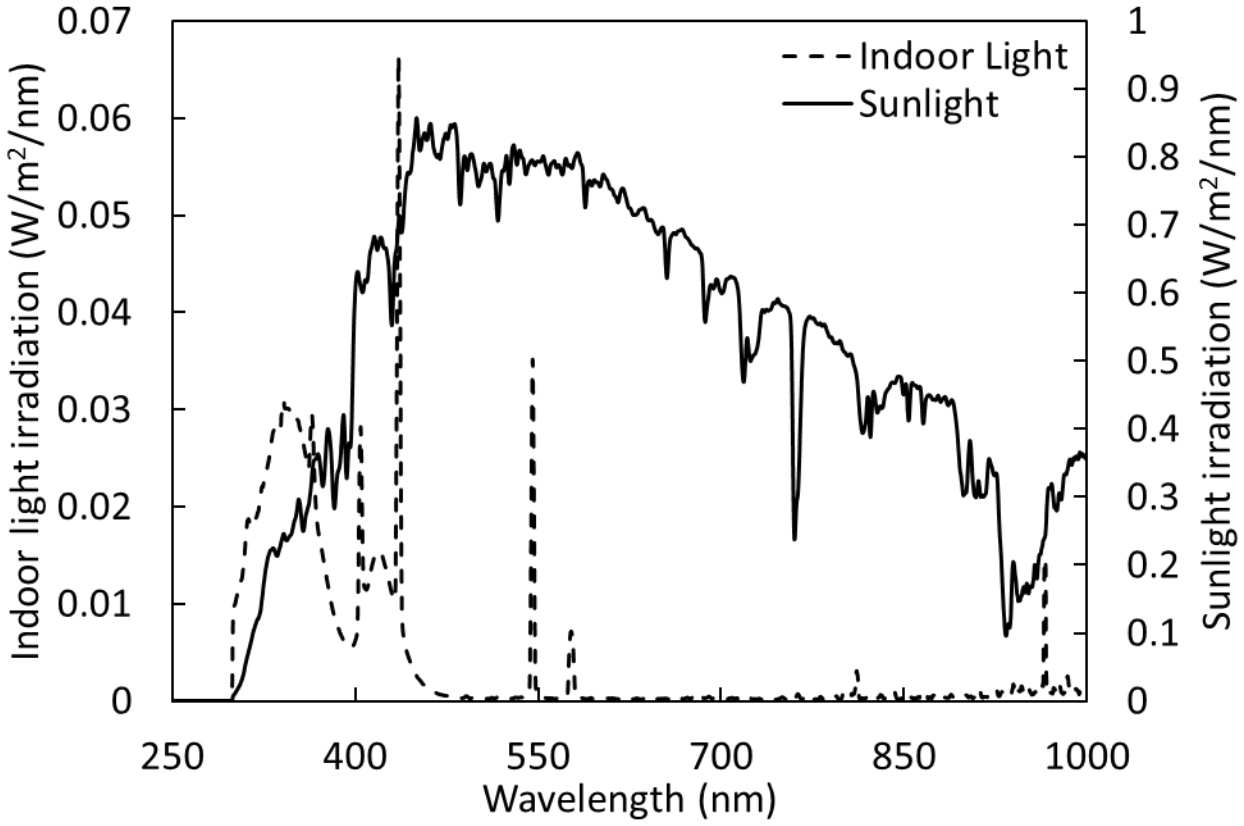

Figure S1. Light irradiation of the indoor–UV light and the sunlight measured with a fibro–optical portable spectrometer (EPP2000, Stellar Net Inc., USA). The sunlight irradiance was measured on April 20th, 2016 in University of Florida Atmospheric Photochemical Outdoor Reactor, Florida, USA (latitude/longitude: 29.64185°/-82.347883°).

Figure S2

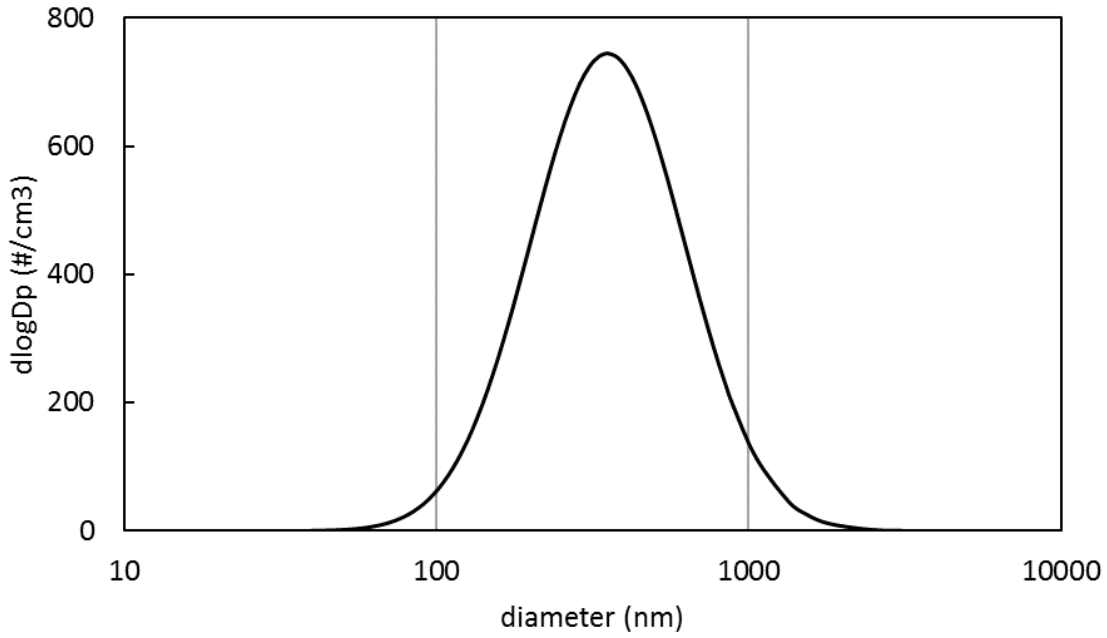

Figure S2. Typical particle size distribution of Arizona Test Dust particles for dust concentration of 74 μg m^3 for the experiment on November 22, 2016. The particle number concentration was measured by combining a scanning mobility particle sizer (SMPS, TSI 3080, USA) and an Optical Particle Counter (OPC, TSI 3330, USA) using a Multi–instrument Manager (MIM2^{TM}) Software provided by TSI.

Figure S3

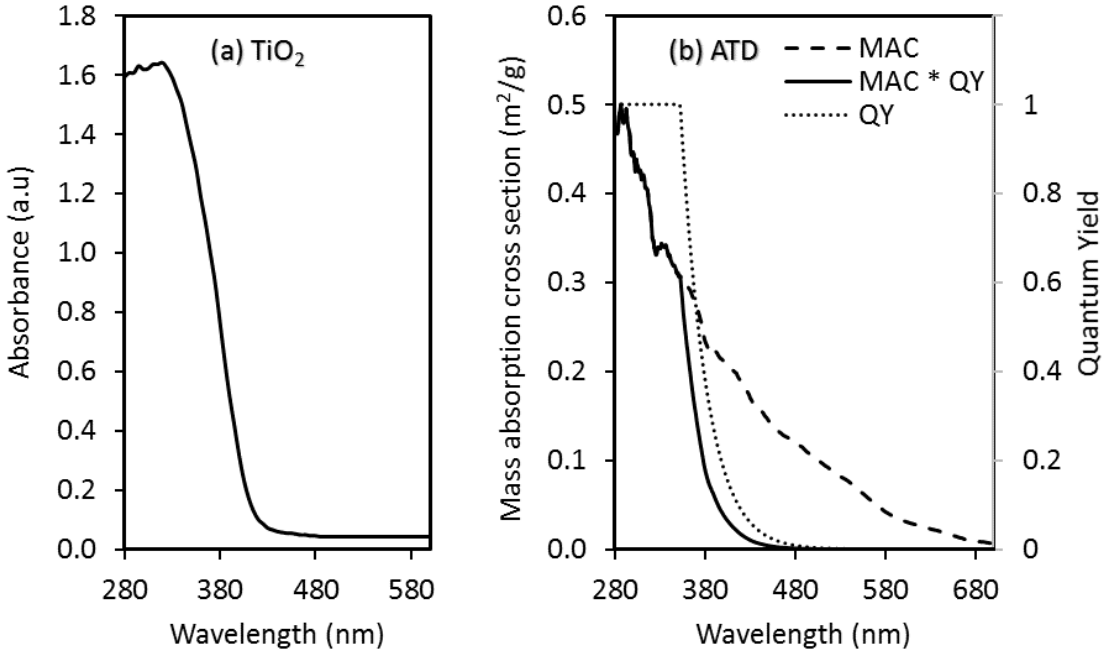

Figure S3. (a) Light absorption of TiO_2 (Reyes–Coronado et al., 2008) (b) The mass absorption cross section (MAC) and the quantum yield (QY) of Arizona Test Dust particles were multiplied to calculate the photocatalytic rate coefficient. The quantum yield of Arizona Test Dust particles was derived from the absorption spectrum of TiO_2.

Figure S4

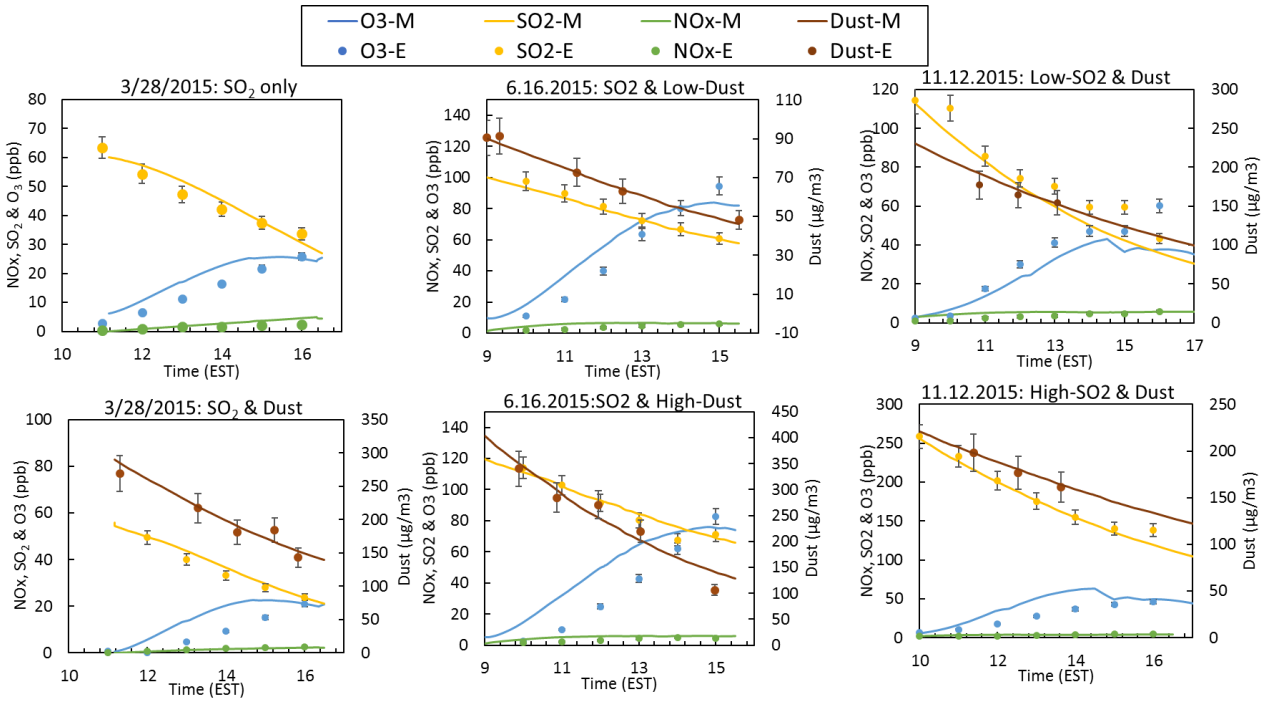

Figure S4. Simulated Ozone, NO_x, SO_2, and Dust concentration compare to outdoor experimental observation for Outdoor experiment (3/28/2015, 6/16/2015 and 11/12/2015). "E" denotes the experimentally observation and "M" denotes the model–predicted concentration of trace gases as well as ATD particles. All the simulations included the chamber dilution and the wall process of gaseous compounds and particles. The errors associated with the observation of SO_2, NO_x, O_3 and dust particle mass concentration were ±0.9%, ±12.5%, ±0.2% and ±6%, respectively.

Figure S5

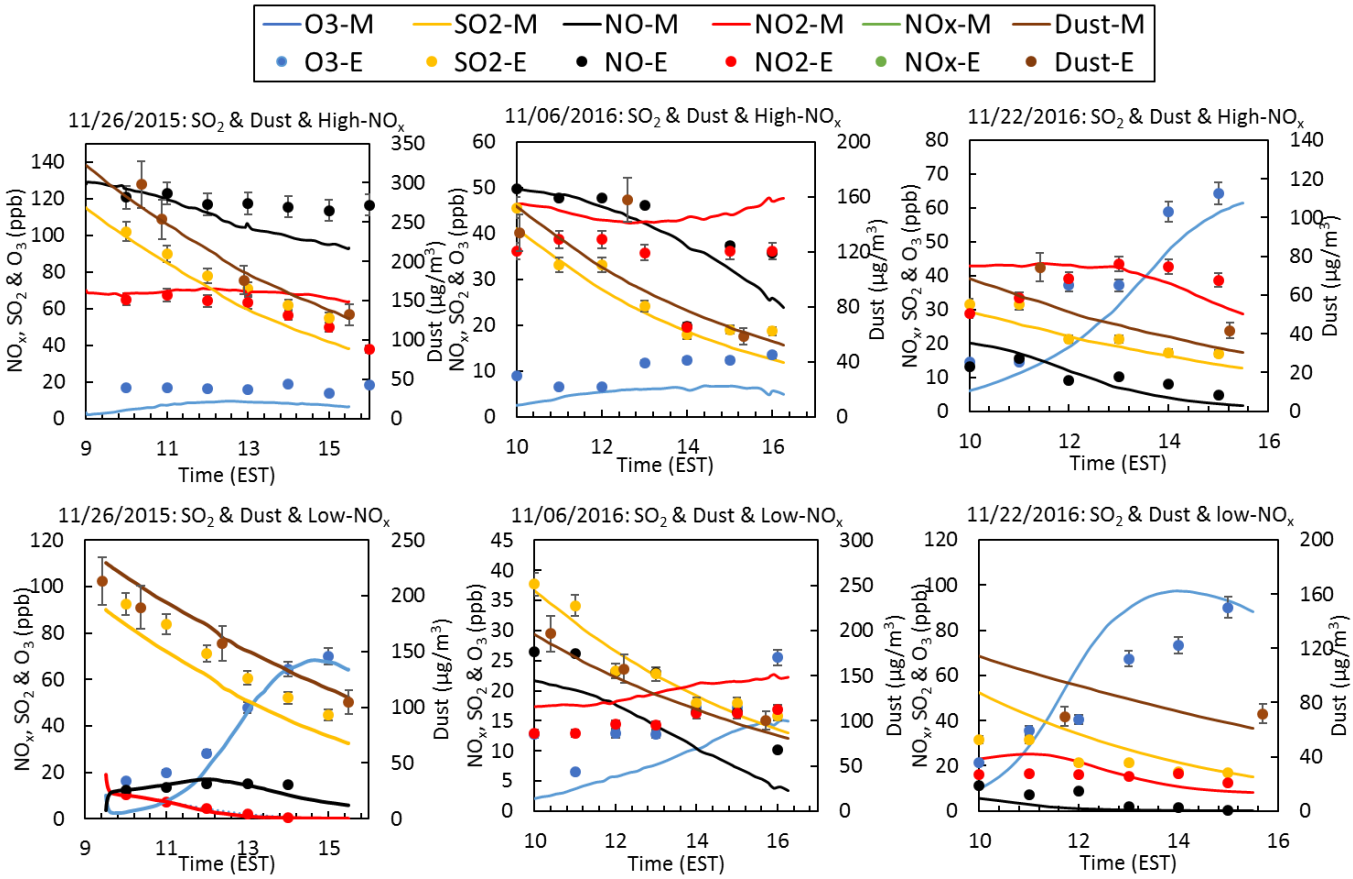

Figure S5. Simulated Ozone, NO_x, SO_2, and Dust concentration compare to outdoor experimental observation for Outdoor experiment (5/11/2015 and 11/26/2015). "E" denotes the experimentally observation and "M" denotes the model–predicted concentration of trace gases and ATD particles. All the simulations included the chamber dilution and the wall process of gaseous compounds and particles. The errors associated with the observation of SO_2, NO, NO_2, O_3 and dust particle mass concentration were ±0.9%, ±12.5%, ±6.9%, ±0.2% and ±6%, respectively.

Figure S6

(a) Total solar UV radiation

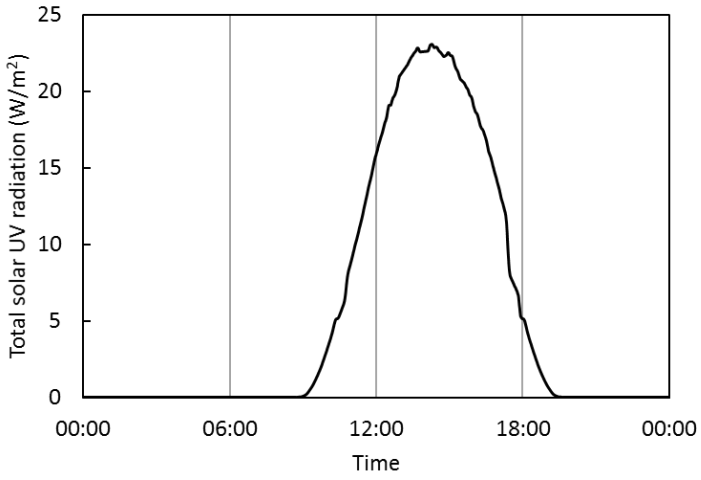

(b) Temperature and humidity

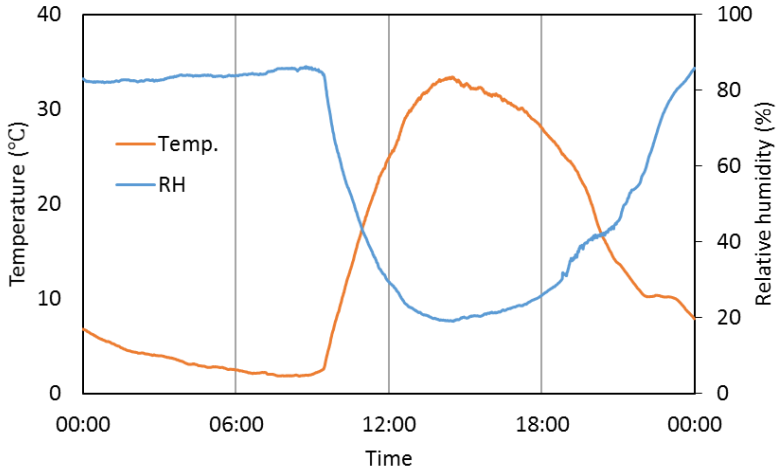

Figure S6. Time profile of (a) total solar UV irradiation and (b) temperature and humidity measured on November 22, 2016 at University of Florida Atmospheric Photochemical Outdoor Reactor, Florida, USA (latitude/longitude: 29.64185°/–82.347883°). The total solar short–wave radiation (0.295 to 0.385 μm) was measured using an ultraviolet radiometer (TUVR, Eppley Laboratory Inc.) inside the chamber. The temperature and humidity are continuously monitored inside the chamber using a hygrometer (CR1000 Measurement and Control System, Campbell Scientific)

Figure S7

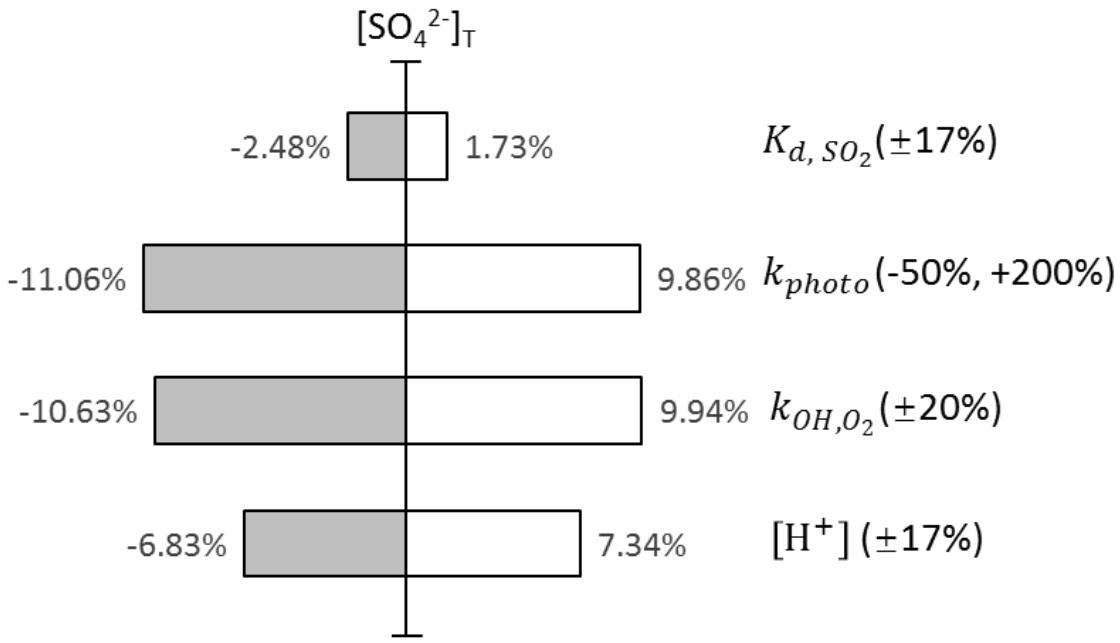

Figure S7. The uncertainty of simulated total sulfate to the variation of selected model parameters. The percent change of the total sulfate was simulated using AMAR model after each parameter was increased or decreased by a factor chosen from the error associated with the parameter. The chamber simulation is conducted with 100 ppb of initial SO_2, 2 ppb of initial NO_2, 2 ppb of initial O_3 and 200 μg m^{-3} of ATD particles at T = 298K and RH = 40% under ambient sunlight on November 22, 2016. NO_x (rate of flux = 2.7×10^6, s^{-1}) and isoprene (2.7×10^6, s^{-1}) were constantly added to chamber for the dilution effects. The simulation was performed without considering the particle loss to the chamber wall.

Figure S8

(a) Rural area

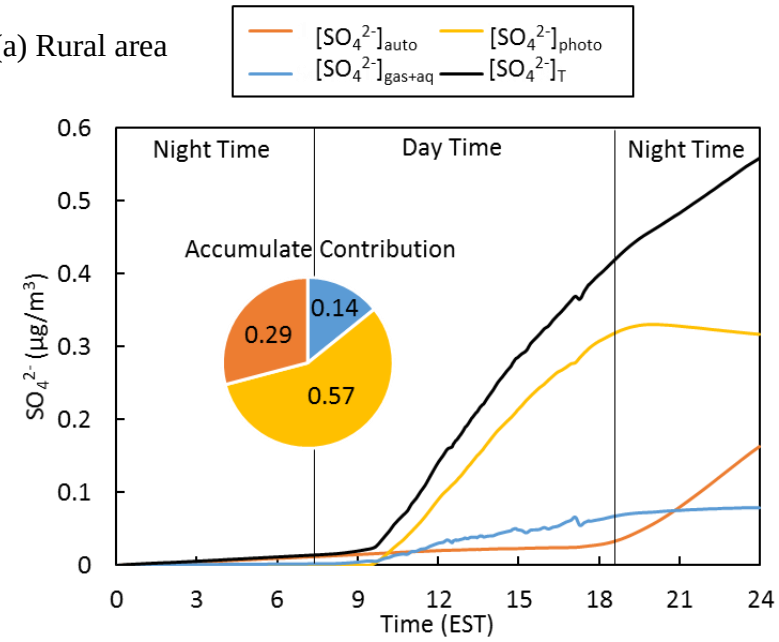

(b) Urban area

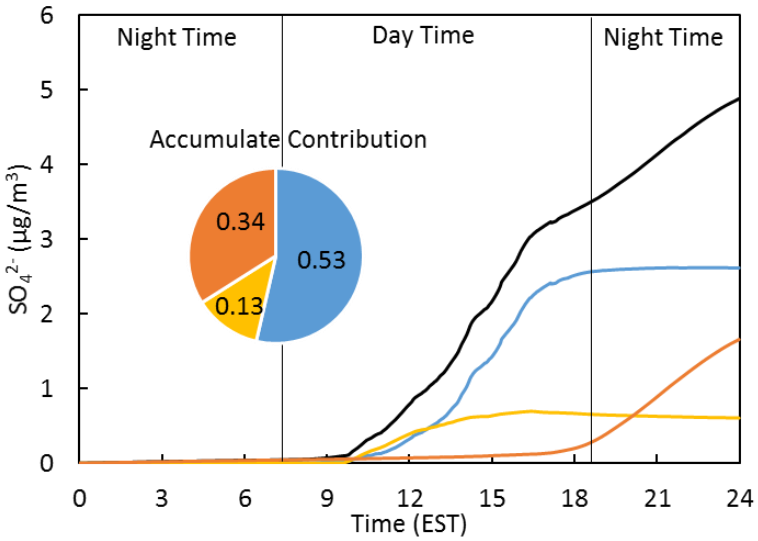

Figure S8. 24 hours simulation of attribution of sulfate formation under the rural (Fig. S8(a)) and polluted urban environment (Fig. S8(b)) using AMAR model. The total sulfate is simulated to show the composition including the sulfate formed from non–dust chemistry ($[SO_4^{2-}]_{aq}$+$[SO_4^{2-}]_{gas}$), from dust–phase autoxidation ($[SO_4^{2-}]_{auto}$), and from dust photochemistry ($[SO_4^{2-}]_{photo}$). The meteorological parameters (i.e., temperature and humidity) are obtained from outdoor chamber experiment (11.22.2016, Table 2). The particle loss to the chamber wall was not considered into the simulation while the dilution process was included.

In Fig. S8(a), 200 μg m^{-3} of ATD particles, 2 ppb of initial SO_2, 5 ppb of NO_x and 20 ppb of isoprene were set for the simulation of rural condition.

In Fig. S8(b), 200 μg m^{-3} of ATD particles, 30 ppb of initial SO_2, 40 ppb of NO_x and 30 ppb of isoprene were set for the simulation of polluted condition.

Table S1. Chemical mechanism for AMAR model

	Reaction	Rate constant [a]	Note
	gas phase [b]		
1	$O^3P + SO_2 \rightarrow SO_3$	$9.75\times10^{-13}\exp(-2280/T)$	Baulch et al., 1984; Kerr, 1984
2	$HO_2 + SO_2 \rightarrow SO_3 + OH\cdot$	1.00×10^{-18}	Atkinson et al., 1989; Atkinson and Lloyd, 1984
3	$CH_3\text{-}O_2\cdot + SO_2 \rightarrow SO_3 + CH_3\text{-}O\cdot$	5.00×10^{-17}	Atkinson et al., 1989; Atkinson and Lloyd, 1984
4	$CH_3\text{-}O\cdot + SO_2 \rightarrow CH_3\text{-}O\text{-}SO_2\cdot$	5.50×10^{-13}	Calvert, 1983
5	$CH_3\cdot + SO_2 \rightarrow CH_3(O)S(O)\cdot$	2.90×10^{-13}	Graedel, 1977
6	$SO_2 + h\upsilon \rightarrow SO_2^*$	$2\times j[NO_2_to_O^3P]$	Graedel, 1977
7	$OH\cdot + SO_2 \rightarrow HOSO_2$	$9.07\times10^{-13}\exp(231/T)$	Atkinson et al., 1989; Kerr, 1984
8	$NO_2 + SO_2 \rightarrow NO + SO_3$	2.00×10^{-26}	Sander, 2006
9	$NO_3 + SO_2 \rightarrow NO_2 + SO_3$	7.00×10^{-21}	Sander, 2006
10	$CH_3\text{-}SO_3\cdot \rightarrow SO_3 + CH_3\cdot$	4.00×10^{-2}	Chen and Jang, 2012
11	$CH_3\text{-}SO_3\cdot + H\text{-}CO\text{-}H \rightarrow CH_3\text{-}SO_3H + HO_2\cdot + CO$	1.60×10^{-15}	Yin et al., 1990
12	$CH_3\text{-}SO_3\cdot + HO_2 \rightarrow CH_3\text{-}SO_3H + O_2$	5.00×10^{-11}	Yin et al., 1990
13	$CH_3\text{-}SO_3\cdot + HONO \rightarrow CH_3\text{-}SO_3H + NO_2$	6.60×10^{-16}	Yin et al., 1990
14	$CH_3\text{-}SO_3\cdot + H_2O_2 \rightarrow CH_3\text{-}SO_3H + HO_2\cdot$	3.00×10^{-16}	Yin et al., 1990
15	$CH_3\text{-}SO_3\cdot + CH_3\text{-}OOH \rightarrow CH_3\text{-}SO_3H + CH_3\text{-}O_2\cdot$	3.00×10^{-16}	Yin et al., 1990
16	$CH_3\text{-}SO_3\cdot + CH_3\text{-}OH \rightarrow CH_3\text{-}SO_3H + H\text{-}CO\text{-}H + HO_2\cdot$	1.00×10^{-16}	Yin et al., 1990
17	$CH_3\text{-}SO_3\cdot + NO_2 \rightarrow CH_3(O)S(O)ONO_2$	3.00×10^{-15}	Yin et al., 1990
18	$CH_3(O)S(O)ONO_2 + H_2O \rightarrow CH_3\text{-}SO_3H + HNO_3$	1.00×10^{-15}	Yin et al., 1990
19	$CH_3\text{-}SO_3\cdot + NO \rightarrow CH_3(O)S(O)ONO$	3.00×10^{-15}	Yin et al., 1990
20	$CH_3(O)S(O)ONO + H_2O \rightarrow CH_3\text{-}SO_3H + HONO$	1.00×10^{-15}	Yin et al., 1990
21	$CH_3(O)S(O)\cdot + NO_2 \rightarrow CH_3\text{-}SO_3\cdot + NO$	5.00×10^{-13}	Chen and Jang, 2012
22	$CH_3(O)S(O)\cdot O_3 \rightarrow CH_3\text{-}SO_3\cdot + O_2$	5.00×10^{-15}	Yin et al., 1990

Table S1. (continued)

	Reaction	Rate constant [a]	Note
23	$CH_3(O)S(O)\cdot + HO_2 \rightarrow CH_3\text{-}SO_3\cdot + OH$	2.50×10^{-13}	Yin et al., 1990
24	$CH_3(O)S(O)\cdot \rightarrow CH_3\cdot + SO_2$	1.00×10^{1}	Mellouki et al., 1988
25	$CH_3(O)S(O)\cdot + O_2 \rightarrow CH_3(O)S(O)OO\cdot$	2.60×10^{-18}	Yin et al., 1990
26	$CH_3(O)S(O)OO\cdot \rightarrow CH_3(O)S(O)\cdot + O_2$	3.30	Yin et al., 1990
27	$CH_3(O)S(O)\cdot + NO_3 \rightarrow CH_3\text{-}SO\cdot + NO_2$	1.00×10^{-14}	Yin et al., 1990
28	$CH_3(O)S(O)\cdot + CH_3\text{-}O_2\cdot \rightarrow CH_3\text{-}SO_3\cdot + CH_3\text{-}O\cdot$	2.50×10^{-13}	Yin et al., 1990
29	$CH_3(O)S(O)\cdot + CH_3\text{-}S\cdot \rightarrow CH_3(O)S(O)S\text{-}CH_3$	4.20×10^{-11}	Yin et al., 1990
30	$CH_3(O)S(O)\cdot + CH_3(O)S(O)\cdot \rightarrow CH_3\text{-}SO\cdot + CH_3\text{-}SO_3\cdot$	7.50×10^{-12}	Yin et al., 1990
31	$CH_3(O)S(O)\cdot + CH_3\text{-}S\text{-}NO\cdot \rightarrow CH_3(O)S(O)CH_3 + NO$	6.80×10^{-13}	Yin et al., 1990
32	$CH_3(O)S(O)\cdot + OH\cdot \rightarrow CH_3\text{-}SO_3H$	5.00×10^{-11}	Yin et al., 1990
33	$CH_3(O)S(O)OO\cdot + NO \rightarrow CH_3\text{-}SO_3\cdot + NO_2$	1.00×10^{-11}	Yin et al., 1990
34	$CH_3(O)S(O)OO\cdot + NO_2 \rightarrow CH_3(O)S(O)OONO_2$	1.00×10^{-12}	Yin et al., 1990
35	$CH_3(O)S(O)OONO_2 \rightarrow CH_3(O)S(O)OO\cdot + NO_2$	4.20×10^{-03}	Yin et al., 1990
36	$CH_3(O)S(O)OO\cdot + CH_3\text{-}S\cdot \rightarrow CH_3\text{-}SO_3\cdot + CH_3\text{-}SO\cdot$	6.00×10^{-11}	Yin et al., 1990
37	$CH_3(O)S(O)OO\cdot + CH_3\text{-}SO\cdot \rightarrow CH_3\text{-}SO_3\cdot + CH_3(O)S(O)\cdot$	8.00×10^{-12}	Yin et al., 1990
38	$CH_3(O)S(O)OO\cdot + CH_3(O)S(O)\cdot \rightarrow 2CH_3\text{-}SO_3\cdot$	3.00×10^{-13}	Yin et al., 1990
39	$CH_3(O)S(O)OO\cdot + HO_2\cdot \rightarrow CH_3(O)S(O)OOH\cdot + O_2$	2.00×10^{-12}	Yin et al., 1990
40	$CH_3(O)S(O)OO\cdot + CH_3\text{-}O_2 \rightarrow CH_3\text{-}SO_3\cdot + CH_3\text{-}O\cdot + O_2$	5.50×10^{-12}	Yin et al., 1990
41	$CH_3(O)S(O)OO\cdot + CH_3(O)S(O)OO\cdot + CH_3\text{-}SO\cdot \rightarrow 2CH_3\text{-}SO_3\cdot + O_2$	6.00×10^{-12}	Yin et al., 1990
42	$CH_3(O)S(O)OO\cdot + CH_3\text{-}S\text{-}OH \rightarrow CH_3(O)S(O)OOH + CH_3\text{-}SO\cdot$	4.00×10^{-13}	Yin et al., 1990
43	$CH_3\text{-}SO\cdot + O_2 \rightarrow CH_3\text{-}S(O)OO\cdot$	7.70×10^{-18}	Yin et al., 1990
44	$CH_3\text{-}S(O)OO\cdot \rightarrow CH_3\text{-}SO\cdot + O_2$	1.70×10^{2}	Yin et al., 1990
45	$CH_3\text{-}SO\cdot + NO_2 \rightarrow CH_3(O)S(O)\cdot + NO$	6.00×10^{-12}	MCM v3.3
46	$CH_3\text{-}SO\cdot + NO_2 \rightarrow CH_3\cdot + NO + SO_2$	3.00×10^{-12}	MCM v3.3
47	$CH_3\text{-}SO\cdot \rightarrow SO\cdot + CH_3\cdot$	2.66×10^{32} exp(-25200/T)	Yin et al., 1990
48	$CH_3\text{-}SO\cdot + NO_3\cdot \rightarrow CH_3(O)S(O)\cdot + NO_2$	8.00×10^{-12}	Yin et al., 1990
49	$CH_3\text{-}SO\cdot + O_3 \rightarrow CH_3(O)S(O)\cdot + O_2$	1.00×10^{-12}	Tyndall and Ravishankara, 1989

Table S1. (continued)

	Reaction	Rate constant [a]	Note
51	$CH_3\text{-}SO\cdot + CH_3\text{-}SO\cdot \rightarrow CH_3\text{-}SO\cdot + CH_3(O)S(O)\cdot$	7.50×10^{-12}	Yin et al., 1990
50	$CH_3\text{-}SO\cdot + HO_2 \rightarrow CH_3(O)S(O)\cdot + OH$	1.50×10^{-12}	Yin et al., 1990
52	$CH_3\text{-}SO\cdot + CH_3\text{-}O_2 \rightarrow CH_3(O)S(O)\cdot + CH_3\text{-}O\cdot$	3.00×10^{-12}	Yin et al., 1990
53	$CH_3\text{-}SO\cdot + CH_3\text{-}NO \rightarrow CH_3\text{-}S\text{-}(O)CH_3\cdot + NO$	6.80×10^{-13}	Yin et al., 1990
54	$CH_3\text{-}SO\cdot + OH \rightarrow CH_3\text{-}S(O)OH$	5.00×10^{-11}	Yin et al., 1990
55	$CH_3\text{-}SO\cdot + O_3 \rightarrow SO_2 + CH_3\text{-}O_2$	3.20×10^{-13}	Borissenko et al., 2003
56	$CH_3\text{-}S\cdot + O_2 \rightarrow CH_3\text{-}SOO\cdot$	5.80×10^{-17}	Sander, 2006
57	$CH_3\text{-}SOO\cdot \rightarrow CH_3\text{-}S\cdot + O_2$	6.00×10^{2}	Yin et al., 1990
58	$CH_3\text{-}S\cdot + O_3 \rightarrow CH_3\text{-}SO\cdot + O_2$	5.70×10^{-12}	Domine et al., 1992
59	$CH_3\text{-}S\cdot + NO_2 \rightarrow CH_3\text{-}S\text{-}NO_2\cdot$	6.10×10^{-13}	Yin et al., 1990
60	$CH_3\text{-}S\cdot + NO_2 \rightarrow CH_3\text{-}SO\cdot + NO$	6.10×10^{-11}	Yin et al., 1990
61	$CH_3\text{-}S\cdot + NO \rightarrow CH_3\text{-}S\text{-}NO\cdot$	2.87×10^{-11}	Balla et al., 1986
62	$CH_3\text{-}S\cdot + NO_3\cdot \rightarrow CH_3\text{-}SO\cdot NO_2$	6.40×10^{-11}	Yin et al., 1990
63	$CH_3\text{-}S\cdot + HO_2\cdot \rightarrow CH_3\text{-}SO\cdot + OH$	3.00×10^{-11}	Yin et al., 1990
64	$CH_3\text{-}S\cdot + CH_3\text{-}O_2\cdot \rightarrow CH_3\text{-}SO\cdot + CH_3\text{-}O\cdot$	6.10×10^{-11}	Yin et al., 1990
65	$CH_3\text{-}S\cdot + CH_3\text{-}S\cdot \rightarrow CH_3\text{-}S\text{-}S\text{-}CH_3$	4.15×10^{-11}	Graham et al., 1964
66	$CH_3\text{-}S\cdot + CH_3\text{-}S\text{-}NO\cdot \rightarrow CH_3\text{-}S\text{-}S\text{-}CH_3 + NO$	1.40×10^{-12}	Yin et al., 1990
67	$CH_3\text{-}S\cdot + OH\cdot \rightarrow CH_3\text{-}S\text{-}OH$	5.00×10^{-11}	Yin et al., 1990
68	$CH_3\text{-}S\text{-}NO\cdot + h\nu \rightarrow CH_3\text{-}S\cdot + NO$	$0.5\times j[NO_2_to_O^3P]$	Yin et al., 1990
69	$CH_3\text{-}S\cdot + O_3 \rightarrow SO_2 + CH_3\text{-}O\cdot$	5.70×10^{-12}	Domine et al., 1992
70	$CH_3\text{-}S\cdot + CH_3\text{-}S\text{-}CH_3 + (O_2) \rightarrow CH_3 + CH_3\text{-}S(O)CH_3 + SO\cdot$	8.00×10^{-12}	Chen and Jang, 2012
71	$CH_3\text{-}S(O)OH + OH\cdot \rightarrow CH_3(O)S(O)\cdot + H_2O$	1.16×10^{-10}	Kukui et al., 2003
72	$CH_3\text{-}S(O)OH + CH_3\text{-}SO_3\cdot \rightarrow CH_3(O)S(O)\cdot + CH_3\text{-}SO_3H$	2.00×10^{-13}	Yin et al., 1990
73	$CH_3\text{-}S(O)OH + CH_3\text{-}O\cdot \rightarrow CH_3(O)S(O)\cdot + CH_3\text{-}OH$	1.00×10^{-13}	Yin et al., 1990
74	$CH_3\text{-}S(O)OH + O^3P \rightarrow CH_3(O)S(O)\cdot + OH\cdot$	1.00×10^{-13}	Yin et al., 1990
75	$CH_3\text{-}S(O)OH + NO_3 \rightarrow CH_3(O)S(O)\cdot + HNO_3$	1.00×10^{-13}	Yin et al., 1990
76	$CH_3\text{-}S(O)OH + HO_2 \rightarrow CH_3(O)S(O)\cdot + H_2O_2$	1.00×10^{-15}	Yin et al., 1990

Table S1. (continued)

	Reaction	Rate constant [a]	Note
77	$CH_3\text{-}S(O)OH + CH_3\text{-}O_2\cdot \rightarrow CH_3(O)S(O)\cdot + CH_3\text{-}OOH$	1.00×10^{-15}	Yin et al., 1990
78	$CH_3\text{-}S\text{-}S\text{-}CH_3 + OH\cdot \rightarrow CH_3\text{-}S\text{-}OH + CH_3\text{-}S\cdot$	5.59×10^{-11} exp(380/T)	Atkinson et al., 1989
79	$CH_3\text{-}S\text{-}S\text{-}CH_3 + O^3P \rightarrow CH_3\text{-}SO\cdot + CH_3\text{-}S\cdot$	5.62×10^{-11} exp(250/T)	Atkinson et al., 1989; Cvetanovic et al., 1981; Nip et al., 1981
80	$CH_3\text{-}S\text{-}S\text{-}CH_3 + NO_3 \rightarrow CH_3\text{-}S(ONO_2)S\text{-}CH_3$	7.00×10^{-13}	Yin et al., 1990
81	$CH_3\text{-}S(ONO_2)S\text{-}CH_3 \rightarrow CH_3\text{-}S(O)NO_2\cdot + CH_3\text{-}S\cdot$	1.00×10^{2}	Yin et al., 1990
82	$CH_3\text{-}S\text{-}S\text{-}CH_3 + h\nu \rightarrow 2CH_3\text{-}S\cdot$	$5.0\times10^{-3}\times j[NO_2_to_O^3P]$	Yin et al., 1990
83	$CH_3\text{-}S(O)NO_2\cdot \rightarrow CH_3\text{-}SO\cdot + NO_2$	1.00	Yin et al., 1990
84	$SO_2^* \rightarrow SO_2$	3.70×10^{6}	Graedel, 1977
85	$SO_2^* + SO_2 \rightarrow SO + SO_3$	6.30×10^{-13}	Graedel, 1977
86	$SO_2^* + CO \rightarrow SO + CO_2$	1.10×10^{-14}	Graedel, 1977
87	$HOSO_2 + O_2 \rightarrow HO_2 + SO_3$	4.00×10^{-13}	Atkinson et al., 1989; Kerr, 1984
88	$HOSO_2 + OH\cdot + M \rightarrow H_2SO_4 + M$	1.00×10^{-11}	Graedel, 1979
89	$SO_3 + H_2O + M \rightarrow H_2SO_4 + M$	9.10×10^{-13}	Atkinson and Lloyd, 1984; Kerr, 1984
90	$SO_3 + O^3P \rightarrow SO_2 + O_2$	7.00×10^{-13}	Calvert et al., 1978
91	$SO\cdot + O_2 \rightarrow SO_2 + O^3P\cdot$	1.39×10^{-13}exp(-2280/T)	Atkinson et al., 1989
92	$SO\cdot + NO_2 \rightarrow SO_2 + NO$	1.40×10^{-11}	Atkinson et al., 1989
93	$SO\cdot + O_3 \rightarrow SO_2 + O_2$	4.51×10^{-12}exp(-1170/T)	Atkinson et al., 1989
94	$SO\cdot + O^3P \rightarrow SO_2$	2.20×10^{-11}	Graedel, 1977
95	$SO\cdot + OH \rightarrow SO_2 + HO_2$	1.10×10^{-10}	Graedel, 1977
96	$SO\cdot + SO_3 \rightarrow 2SO_2$	2.00×10^{-15}	Graedel, 1977
	Aqueous phase [c]		
1	$OH(aq) + HO_2(aq) \rightarrow H_2O(aq) + O_2(aq)$	1.01×10^{12}exp(-1500/T)/V	Sehested et al., 1968; Thomas, 1963
2	$OH(aq) + O_2^- \rightarrow O_2(aq) + OH^-$	1.30×10^{12}exp(-1500/T)/V	Buxton et al., 1988
3	$HO_2(aq) + O_2^- \rightarrow H_2O_2(aq) + O_2(aq) + OH^-$	3.29×10^{9}exp(-1050/T)/V	Bielski et al., 1985

Table S1. (continued)

	Reaction	Rate constant [a]	Note
4	$HO_2(aq) + HO_2(aq) \rightarrow H_2O_2(aq) + O_2(aq)$	$7.14\times10^{9}\exp(-2700/T)/V$	Bielski et al., 1985
5	$OH(aq) + H_2O_2(aq) \rightarrow HO_2(aq) + H_2O(aq)$	$8.11\times10^{9}\exp(-1700/T)/V$	Christensen et al., 1982; Buxton et al., 1988
6	$O_2^- + O_3(aq) \rightarrow OH(aq) + OH^- + 2O_2(aq)$	$2.30\times10^{11}\exp(-1500/T)/V$	Sehested et al., 1983; Bielski et al., 1985;
7	$H_2O_2(aq) + h\nu \rightarrow OH(aq) + OH(aq)$	$j[H_2O_2_to_OH]$	Lin et al., 1978; Molina et al., 1981; Nicovich et al., 1988; Vaghjiani et al., 1989
8	$OH(aq) + HSO_3^- \rightarrow SO_5^- + H_2O(aq)$	$6.91\times10^{11}\exp(-1500/T)/V$	Huie and Neta, 1987
9	$HSO_3^- + H^+ + H_2O_2(aq) \rightarrow SO_4^{2-} + 2H^+$	$5.77\times10^{14}\exp(-4725/T)/V$	Hoffmann and Calvert, 1985
10	$SO_3^{2-} + H^+ + H_2O_2(aq) \rightarrow SO_4^{2-} + H^+$	$5.77\times10^{14}\exp(-4725/T)/V$	Hoffmann and Calvert, 1985
11	$H_2C(OH)_2 + OH(aq) \rightarrow HO_2(aq) + HCOOH(aq)$	$2.21\times10^{10}\exp(-1000/T)/V$	Chin and Wine, 1994
12	$OH(aq) + SO_3^{2-} \rightarrow SO_5^- + OH^-$	$8.44\times10^{11}\exp(-1500/T)/V$	Huie and Neta, 1987; Adams and Boag, 1964; Buxton et al., 1988
13	$HCOO^- + OH(aq) \rightarrow CO_2 + HO_2(aq) + OH^-$	$2.12\times10^{11}\exp(-1250/T)/V$	Chin and Wine, 1994
14	$HSO_3^- + H^+ + CH_3OOH(aq) \rightarrow SO_4^{2-} + 2H^+ + CH_3OH(aq)$	$6.13\times10^{12}\exp(-3780/T)/V$	Hoffmann and Calvert, 1985
15	$SO_3^{2-} + SO_4^- \rightarrow SO_4^{2-} + SO_5^-$	$1.15\times10^{11}\exp(-1500/T)/V$	Wine et al., 1989
16	$HSO_3^- + SO_4^- \rightarrow SO_4^{2-} + SO_5^- + H^+$	$1.15\times10^{11}\exp(-1500/T)/V$	Wine et al., 1989
17	$HSO_3^- + H_2C(OH)_2 \rightarrow HOCH_2SO_3^-$	$1.01\times10^{4}\exp(-3000/T)/V$	Boyce and Hoffmann, 1984
18	$SO_3^{2-} + H_2C(OH)_2 \rightarrow HOCH_2SO_3^- + OH^-$	$5.21\times10^{7}\exp(-2450/T)/V$	Boyce and Hoffmann, 1984
19	$HSO_3^- + O_3(aq) \rightarrow SO_4^{2-} + H^+$	$3.83\times10^{13}\exp(-5500/T)/V$	Hoffmann and Calvert, 1985
20	$SO_3^{2-} + O_3(aq) \rightarrow SO_4^{2-}$	$7.43\times10^{16}\exp(-5280/T)/V$	Hoffmann and Calvert, 1985
21	$SO_4^- + OH^- \rightarrow SO_4^{2-} + OH(aq)$	$1.23\times10^{10}\exp(-1500/T)/V$	Maruthamuthu and Neta, 1978
22	$SO_4^- + H_2O_2(aq) \rightarrow SO_4^{2-} + H^+ + HO_2(aq)$	$9.86\times10^{9}\exp(-2000/T)/V$	Wine et al., 1989
23	$SO_4^- + H_2O(aq) \rightarrow SO_4^{2-} + H^+ + OH(aq)$	$2.19\times10^{5}\exp(-1850/T)/V$	Bao and Barker, 1996
24	$SO_4^-HCOO^- \rightarrow SO_4^{2-} + CO_2(aq) + OH_2(aq)$	$1.69\times10^{10}\exp(-1500/T)/V$	Wine et al., 1989
25	$CH_3O_2(aq) + O_2^- \rightarrow CH_3OOH(aq) + OH^- + O_2(aq)$	$1.70\times10^{9}\exp(-1050/T)/V$	Jacob, 1986

Table S1. (continued)

	Reaction	Rate constant [a]	Note
26	$HCOOH(aq) + OH(aq) \rightarrow H_2O(aq) + CO_2(aq) + HO_2(aq)$	$3.15\times10^{9}\exp(-1000/T)/V$	Chin and Wine, 1994
27	$O_3(aq) + H_2O_2(aq) + OH^- \rightarrow OH(aq) + O_2^- + O_2(aq) + H_2O(aq)$	$2.97\times10^{14}\exp(-4000/T)/V$	Staehelin and Hoigne, 1982
28	$HOCH_2SO_3^- + OH^- \rightarrow SO_3^{2-} + H_2C(OH)_2$	$1.34\times10^{10}\exp(-4500/T)/V$	Deister et al., 1986; Munger et al., 1986
29	$CH_3OOH(aq) + OH(aq) \rightarrow H_2C(OH)_2(aq) + OH(aq)$	$9.44\times10^{9}\exp(-1850/T)/V$	Jacob, 1986
30	$CH_3OOH(aq) + OH(aq) \rightarrow CH_3O_2(aq) + H_2O(aq)$	$8.11\times10^{9}\exp(-1700/T)/V$	Jacob, 1986
31	$HOCH_2SO_3^- + OH(aq) \rightarrow H_2C(OH)_2(aq) + SO_5^- + H^+ + OH^-$	$2.00\times10^{11}\exp(-1500/T)/V$	Martin et al., 1989
32	$SO_4^- + HO_2(aq) \rightarrow SO_4^{2-} + H^+ + O_2(aq)$	$7.67\times10^{11}\exp(-1500/T)/V$	Jacob, 1986
33	$SO_4^- + O_2^- \rightarrow SO_4^{2-} + O_2(aq)$	$7.67\times10^{11}\exp(-1500/T)/V$	Jacob, 1986
34	$HCOO^- + O_3(aq) \rightarrow CO_2(aq) + OH(aq) + O_2^-$	$1.04\times10^{10}\exp(-5500/T)/V$	Hoigne and Bader, 1983
35	$SO_5^- + HCOO^- \rightarrow HSO_5^- + CO_2(aq) + O_2^-$	$9.45\times10^{9}\exp(-4000/T)/V$	Jacob, 1986
36	$SO_4^- + NO_2^- \rightarrow SO_4^{2-} + NO_2(aq)$	$1.50\times10^{11}\exp(-1500/T)/V$	Wine et al., 1989
37	$SO_5^- + HSO_3^- \rightarrow HSO_5^- + SO_5^-$	$1.02\times10^{10}\exp(-3850/T)/V$	Huie and Neta, 1987
38	$HSO_5^- + OH(aq) \rightarrow SO_5^- + H_2O(aq)$	$9.99\times10^{9}\exp(-1900/T)/V$	Maruthamuthu and Neta, 1977
39	$HSO_5^- + HSO_3^- + H^+ \rightarrow 2SO_4^{2-} + 3H^+$	$1.40\times10^{10}\exp(-2000/T)/V$	McElroy, 1987; Betterton and Hoffmann, 1988a
40	$SO_5^- + HSO_3^- \rightarrow SO_4^- + SO_4^{2-} + H^+$	$9.46\times10^{9}\exp(-3500/T)/V$	Huie and Neta, 1987
41	$O_2^- + SO_5^- \rightarrow O_2(aq) + HSO_5^- + OH^-$	$3.39\times10^{9}\exp(-1050/T)/V$	Jacob, 1986
42	$NO(aq) + NO_2(aq) + H_2O(aq) \rightarrow 2NO_2^- + 2H^+$	$3.07\times10^{10}\exp(-1500/T)/V$	Lee, 1984
43	$NO_2(aq) + NO_2(aq) + H_2O(aq) \rightarrow NO_2^- + 2H^+ + NO_3^-$	$1.53\times10^{10}\exp(-1500/T)/V$	Lee, 1984
44	$NO_2(aq) + OH(aq) \rightarrow NO_3^- + H^+$	$2.00\times10^{11}\exp(-1500/T)/V$	Strehlow and Wagner, 1982
45	$HONO(aq) + h\nu \rightarrow OH(aq) + NO(aq)$	j[HONO_to_OH]	Bongartz et al., 1991; Atkinson et al., 1997
46	$NO_2^- + h\nu \rightarrow OH(aq) + NO(aq)$	j[HONO_to_OH]	Bongartz et al., 1991; Atkinson et al., 1997
47	$HONO(aq) + OH(aq) \rightarrow NO_2(aq) + H_2O(aq)$	$1.53\times10^{11}\exp(-1500/T)/V$	Rettich, 1978
48	$NO_2^- + OH(aq) \rightarrow NO_2(aq) + OH^-$	$1.53\times10^{12}\exp(-1500/T)/V$	Treinin and Hayon, 1970

Table S1. (continued)

	Reaction	Rate constant [a]	Note
49	$HONO(aq) + H_2O_2(aq) + H^+ \rightarrow NO_3^- + H_2O(aq) + 2H^+$	$3.66\times10^{13}\exp(-6700/T)/V$	Lee and Lind, 1986
50	$NO_2^- + O_3(aq) \rightarrow NO_3^- + O_2(aq)$	$6.72\times10^{15}\exp(-6950/T)/V$	Damschen and Martin, 1983
		Gas-aqueous partitioning [d]	
1	$SO_2 \leftrightarrow SO_2(aq)$	$2.66\times10^{-18}\exp(3135/T)\times T/\rho_{in}$	Chameides, 1984
2	$NO_2 \leftrightarrow NO_2(aq)$	$2.34\times10^{-18}\exp(1800/T)\times T/\rho_{in}$	Chameides, 1984
3	$NO \leftrightarrow NO(aq)$	$1.02\times10^{-18}\exp(1500/T)\times T/\rho_{in}$	Schwartz and White, 1981
4	$O_3 \leftrightarrow O_3(aq)$	$3.07\times10^{-19}\exp(2380/T)\times T/\rho_{in}$	Chameides, 1984; Jacob, 1986
5	$H_2O_2 \leftrightarrow H_2O_2(aq)$	$1.48\times10^{-18}\exp(6600/T)\times T/\rho_{in}$	Chameides, 1984; O'Sullivan et al., 1996;
6	$HONO \leftrightarrow HONO(aq)$	$4.80\times10^{-19}\exp(4750/T)\times T/\rho_{in}$	Chameides, 1984; Martin, 1984
7	$HO_2 \leftrightarrow HO_2(aq)$	$3.95\times10^{-20}\exp(6600/T)\times T/\rho_{in}$	Hanson et al., 1992; Jacob, 1986
8	$OH \leftrightarrow OH(aq)$	$4.58\times10^{-20}\exp(5250/T)\times T/\rho_{in}$	Hanson et al., 1992; Jacob, 1986
9	$CH_3O_2 \leftrightarrow CH_3O_2(aq)$	$3.39\times10^{-21}\exp(5600/T)\times T/\rho_{in}$	Jacob, 1986
10	$CH_3CO_2H \leftrightarrow CH_3CO_2H(aq)$	$3.40\times10^{-19}\exp(6400/T)\times T/\rho_{in}$	Lind and Kok, 1986
11	$HCHO \leftrightarrow HCHO(aq)$	$7.79\times10^{-24}\exp(7150/T)\times T/\rho_{in}$	Chameides, 1984; Zhou and Mopper, 1990
12	$CH_3OOH \leftrightarrow CH_3OOH(aq)$	$1.24\times10^{-19}\exp(5600/T)\times T/\rho_{in}$	Lind and Kok, 1986
13	$HCOOH \leftrightarrow HCOOH(aq)$	$1.46\times10^{-18}\exp(5700/T)\times T/\rho_{in}$	Jacob, 1986
		Acid dissociation	
1	$HO_2(aq) \leftrightarrow O_2^- + H^+$	$1.17\times10^{-3}\exp(-1046.4/T)$	Bielski et al., 1985
2	$HCOOH(aq) \leftrightarrow HCOO^- + H^+$	$1.79\times10^{-4}\exp(2.4/T)$	Sillen et al., 1964
3	$HONO(aq) \leftrightarrow NO_2^- + H^+$	$3.07\times10^{-4}\exp(151.6/T)$	Schwartz and White, 1981
4	$SO_2(aq) \leftrightarrow HSO_3^- + H^+$	$2.65\times10^{-2}\exp(-235.7/T)$	Olson and Hoffmann, 1989
5	$HSO_3^-(aq) \leftrightarrow SO_3^{2-} + H^+$	$1.21\times10^{-7}\exp(-180.4/T)$	Olson and Hoffmann, 1989
6	$HCHO(aq) \leftrightarrow H_2C(OH)_2(aq)$	$2.08\times10^{2}\exp(-483.5/T)$	Betterton and Hoffmann, 1988b

Table S1. (continued)

	Reaction	Rate constant [a]	k_1	k_2	k_3	Note
			Gas-dust partitioning [e]			
1	$SO_2 + Dust \rightarrow SO_2(d) + Dust$	f	1×10^{-8}			Adams et al., 2005; Huang et al., 2015
2	$SO_2(d) \rightarrow SO_2$	g	2×10^{9}	3100	0.013	Adams et al., 2005; Huang et al., 2015
3	$O_3 + Dust \rightarrow O_3(d) + Dust$	f	1×10^{-8}			Michel et al. 2003; Underwood et al. 2001
4	$O_3(d) \rightarrow O_3$	h	1×10^{10}	2700		Michel et al. 2003; Underwood et al. 2001
5	$NO_2 + Dust \rightarrow NO_2(d) + Dust$	f	1×10^{-8}			Chameides 1984
6	$NO_2(d) \rightarrow NO_2$	h	5×10^{8}	2500		Chameides 1984
7	$HNO_3 + Dust \rightarrow HNO_3(d) + Dust$	f	1×10^{-8}			Schwartz and White 1981; Schwartz 1984
8	$HNO_3(d) \rightarrow HNO_3$	g	1×10^{15}	8700	15.4	Schwartz and White 1981; Schwartz 1984
9	$HONO + Dust \rightarrow HONO(d) + Dust$	f	1×10^{-8}			Becker et al. 1996
10	$HONO(d) \rightarrow HONO$	g	1×10^{10}	4900	0	Becker et al. 1996
11	$N_2O_5 + Dust \rightarrow HNO_3(d) + Dust$	f	7.3×10^{-3}			Wagner et al. 2009
			Dust phase			
12	$Dust + h\nu \rightarrow Dust + e_h$		$j_{[ATD]}$			estimated
13	$e_h \rightarrow energy$	i	1×10^{-2}			estimated
14	$e_h + O_2 \rightarrow OH(d)$	j	1×10^{-22}	2.3		estimated
15	$SO_2(d) \rightarrow SO_4^{2-}(d)$	i	5×10^{-6}			estimated
16	$SO_2(d) + OH(d) \rightarrow SO_4^{2-}(d)$	i	1×10^{-12}			estimated
17	$SO_2(d) + O_3(d) \rightarrow SO_4^{2-}(d) + O_2$	i	2×10^{-11}			estimated
18	$e_h + O_3(d) \rightarrow OH(d) + O_2$	i	1×10^{-12}			estimated
19	$NO_2(d) \rightarrow NO_3^{-}(d)$	i	6×10^{-5}			estimated
20	$e_h + NO_2(d) \rightarrow HONO(d)$	i	6×10^{-12}			estimated
21	$HONO(d) + h\nu \rightarrow OH(d) + NO$		$j_{[HONO]}$			Stockwell and Calvert, 1978; Atkinson et al., 1997
22	$NO_2(d) + OH(d) \rightarrow NO_3^{-}(d)$	i	1×10^{-10}			estimated

Table S1. (continued)

	Reaction	Rate constant [a]	k_1	k_2	k_3	Note
23	$NO_3^-(d) + Salt(d) \rightarrow NO_3^-(d_salt)$	i	1×10^{-8}			estimated
24	$SO_4^{2-}(d) + Salt(d) \rightarrow SO_4^{2-}(d_salt)$	i	1×10^{-8}			estimated
25	$NO_3^-(d_salt) + SO_4^{2-}(d) \rightarrow SO_4^{2-}(d_salt)$	i	4×10^{-13}			estimated

	Reaction	Rate constant [a]	Note
		Wall loss [k]	
1	$SO_2 \rightarrow$	$(1.3RH + 3.3)\times10^{-6}$	For indoor chamber simulation; measured
2	$O_3 \rightarrow$	7×10^{-5}	For indoor chamber simulation; Chen and Jang, 2012
3	$SO_2 \rightarrow$	$(0.7RH + 1.7)\times10^{-6}$	For outdoor chamber simulation; estimated
4	$O_3 \rightarrow$	3.5×10^{-5}	For outdoor chamber simulation; estimated
5	$Dust \rightarrow$	1×10^{-5}	Measured
6	$SO_4^{2-}(aq) \rightarrow$	5×10^{-6}	Measured

[a] The unit of reaction rate constants is s^{-1} for first-order reactions, cm^3 $molecule^{-1}$ s^{-1} for second-order reactions and cm^6 $molecule^{-2}$ s^{-1} for third order reactions. The unit of the rate constants for the dust sorption reactions is m^3 m^{-2} s^{-1}.

[b] The rate constant parameters of SO_2 oxidation in gas phase are taken from previous studies as shown in note of each reactions and can be also found in Chen and Jang (2012). T (K) is the temperature.

[c] $V = N_A \times V(aq)$, where N_a (6.022×10^{23} molecule mol^{-1}) is the Avogadro constant and V(aq) (L cm^{-3}) is the volume concentration of inorganic salt seeded aqueous phase in the air. The unit of the chemical species in the aqueous phase is mole per cm^3 of air for the model simulation. The rate constant parameters of reactions in aqueous phases are updated from previous studies (Liang et al., 1999). The detailed citation of each reactions was shown in the notes. The concentration of V(aq), H_2O(aq), H^+ and OH^- are calculated using E–AIM II (Clegg et al., 1998;Wexler and Clegg, 2002;Clegg and Wexler, 2011).

[d] The partitioning rate constant of gas to the aqueous phase is derived from Henry constant (mol atm^{-1}). ρ_{in} is the density of the inorganic salt seeded aerosol and is calculated using E–AIM II (Clegg et al., 1998;Wexler and Clegg, 2002;Clegg and Wexler, 2011).

[e] The unit of dust for the model is mass concentration (μg m^{-3}). During simulation, the concentration of dust is multiplied by a factor of 2.45×10^{10} to have same magnitude with other gaseous species.

[f] Rate constant $k = k_1 \sqrt{8\,R\,T/(\pi\,MW)}\, f_{dust,M2S} / 4$, where $f_{dust,M2S} = 3.066 \times 10^{-6}$ (m^2 μg), R = 8.314 is the ideal gas constant and MW is the molecule weight of chemical species.

[g] Rate constant $k = k_1 \exp\left(-\frac{k_2}{T}\right)/(F_{water}(1 + k_3/[H^+]))$, where $F_{water} = \exp(4.4RH) + 3.7\exp(4.4RH)\frac{[NO_3^-]}{[Dust]} + \frac{M_{in,water}}{[Dust]}$. $[H^+]$ and $M_{in,water}$ are the concentration of proton and water in dust phase, respectively, and are dynamically calculated using E–AIM II. (Clegg et al., 1998;Wexler and Clegg, 2002;Clegg and Wexler, 2011).

[h] Rate constant $k = k_1 \exp(-k_2/T)$.

[i] Rate constant $k = k_1$.

[j] Rate constant $k = k_1 \exp(k_2)$.

[k] The wall loss factors for the model simulation are only valid for the indoor and outdoor chambers used this study. The loss factors of gases and particles may be varied for different chamber systems.

Reference

Adams, J. W., Rodriguez, D., and Cox, R. A.: The uptake of SO_2 on Saharan dust: a flow tube study, Atmos. Chem. Phys., 5, 2679–2689, 2005.

Atkinson, R., and Lloyd, A. C.: Evaluation of kinetic and mechanistic data for modeling of photochemical smog, J. Phys. Chem. Ref. Data, 13, 315–444, 1984.

Atkinson, R., Baulch, D., Cox, R., Hampson Jr, R., Kerr, J., and Troe, J.: Evaluated kinetic and photochemical data for atmospheric chemistry: supplement III. IUPAC subcommittee on gas kinetic data evaluation for atmospheric chemistry, J. Phys. Chem. Ref. Data, 18, 881–1097, 1989.

Atkinson, R., Baulch, D., Cox, R., Hampson Jr, R., Kerr, J., Rossi, M., and Troe, J.: Evaluated kinetic and photochemical data for atmospheric chemistry: supplement VI. IUPAC subcommittee on gas kinetic data evaluation for atmospheric chemistry, J. Phys. Chem. Ref. Data, 26, 1329–1499, 1997.

Balla, R. J., Nelson, H., and McDonald, J.: Kinetics of the reaction of CH_3S with NO, NO_2 and O_2, Chem. Phys., 109, 101–107, 1986.

Bao, Z.–C., and Barker, J. R.: Temperature and ionic strength effects on some reactions involving sulfate radical [SO_4^-(aq)], J. Phys. Chem., 100, 9780–9787, 1996.

Baulch, D., Cox, R., Hampson Jr, R., Kerr, J., Troe, J., and Watson, R.: Evaluated kinetic and photochemical data for atmospheric chemistry: supplement II. CODATA task group on gas phase chemical kinetics, J. Phys. Chem. Ref. Data, 13, 1259–1380, 1984.

Becker, K. H., Kleffmann, J., Kurtenbach, R., and Wiesen, P.: Solubility of nitrous acid (HONO) in sulfuric acid solutions, J. Phys. Chem., 100, 14984–14990, 1996.

Betterton, E. A., and Hoffmann, M. R.: Henry's law constants of some environmentally important aldehydes, Environ. Sci. Technol., 22, 1415–1418, 1988a.

Betterton, E. A., and Hoffmann, M. R.: Oxidation of aqueous sulfur dioxide by peroxymonosulfate, J. Phys. Chem., 92, 5962–5965, 1988b.

Bielski, B. H., Cabelli, D. E., Arudi, R. L., and Ross, A. B.: Reactivity of HO_2/O_2^- radicals in aqueous solution, J. Phys. Chem. Ref. Data, 14, 1041–1100, 1985.

Bongartz, A., Kames, J., Welter, F., and Schurath, U.: Near–UV absorption cross sections and trans/cis equilibrium of nitrous acid, J. Phys. Chem., 95, 1076–1082, 1991.

Borissenko, D., Kukui, A., Laverdet, G., and Le Bras, G.: Experimental study of SO_2 formation in the reactions of CH3SO radical with NO_2 and O_3 in relation with the atmospheric oxidation mechanism of dimethyl sulfide, J. Phys. Chem. A, 107, 1155–1161, 2003.

Boyce, S. D., and Hoffmann, M. R.: Kinetics and mechanism of the formation of hydroxymethanesulfonic acid at low pH, J. Phys. Chem., 88, 4740–4746, 1984.

Buxton, G. V., Greenstock, C. L., Helman, W. P., and Ross, A. B.: Critical review of rate constants for reactions of hydrated electrons, hydrogen atoms and hydroxyl radicals (· OH/· O− in aqueous solution, J. Phys. Chem. Ref. Data, 17, 513-886, 1988.

Calvert, J. G., Su, F., Bottenheim, J. W., and Strausz, O. P.: Mechanism of the homogeneous oxidation of sulfur dioxide in the troposphere, Atmos. Environ., 12, 197-226, 1978.

Calvert, J. G., and Stockwell, W.: Mechanism and rates of the gas phase oxidations of sulfur dioxide and the nitrogen oxides in the atmosphere, Ohio State Univ., Columbus (USA). Dept. of Chemistry, 1983.

Chameides, W. L.: The photochemistry of a remote marine stratiform cloud, J. Geophys. Res. Atmos., 89, 4739–4755, 1984.

Chen, T., and Jang, M.: Chamber simulation of photooxidation of dimethyl sulfide and isoprene in the presence of NO_x, Atmos. Chem. Phys., 12, 10257–10269, 2012.

Chin, M., and Wine, P.: A temperature–dependent competitive kinetics study of the aqueous–phase reactions of OH radicals with formate, formic acid, acetate, acetic acid, and hydrated formaldehyde, Aquatic and Surface Photochemistry, 85–96, 1994.

Christensen, H., Sehested, K., and Corfitzen, H.: Reactions of hydroxyl radicals with hydrogen peroxide at ambient and elevated temperatures, J. Phys. Chem., 86, 1588–1590, 1982.

Clegg, S., and Wexler, A. S.: Densities and Apparent Molar Volumes of Atmospherically Important Electrolyte Solutions. 2. The Systems $H^+ - HSO_4^- - SO_4^{2-} - H_2O$ from 0 to 3 mol kg^{-1} as a Function of Temperature and $H^+ - NH_4^+ - HSO_4^- - SO_4^{2-} - H_2O$ from 0 to 6 mol kg^{-1} at 25° C Using a Pitzer Ion Interaction Model, and $NH_4HSO_4^- H_2O$ and $(NH_4)_3H(SO_4)^{2-} H_2O$ over the Entire Concentration Range, J. Phys. Chem. A, 115, 3461–3474, 2011.

Clegg, S. L., Brimblecombe, P., and Wexler, A. S.: Thermodynamic model of the system H^+–NH_4^+–SO_4^{2-}–NO_3^--H_2O at tropospheric temperatures, J. Phys. Chem. A, 102, 2137–2154, 1998.

Cvetanovic, R., Singleton, D., and Irwin, R.: Gas–phase reactions of O (^3P) atoms with methanethiol, ethanethiol, methyl sulfide, and dimethyl disulfide. 2. Reaction products and mechanisms, J. Am. Chem. Soc., 103, 3530–3539, 1981.

Damschen, D. E., and Martin, L. R.: Aqueous aerosol oxidation of nitrous acid by O_2, O_3 and H_2O_2, Atmos. Environ., 17, 2005–2011, 1983.

Deister, U., Neeb, R., Helas, G., and Warneck, P.: Temperature dependence of the equilibrium $CH_2(OH)_2 + HSO_3^- = CH_2(OH)SO_3^- + H_2O$ in aqueous solution, J. Phys. Chem., 90, 3213–3217, 1986.

Domine, F., Ravishankara, A., and Howard, C. J.: Kinetics and mechanisms of the reactions of methylthio, methylsulfinyl, and methyldithio radicals with ozone at 300 K and low pressures, J. Phys. Chem., 96, 2171–2178, 1992.

Graedel, T.: The homogeneous chemistry of atmospheric sulfur, Rev. Geophys., 15, 421–428, 1977.

Graedel, T.: Reduced sulfur emission from the open oceans, Geophys. Res. Lett., 6, 329–331, 1979.

Graham, D., Mieville, R., Pallen, R., and Sivertz, C.: Photo–initiated reactions of thiols and olefins: II. The addition of methanethiol to unconjugated olefins, Can. J. Chem., 42, 2250–2255, 1964.

Hanson, D. R., Burkholder, J. B., Howard, C. J., and Ravishankara, A.: Measurement of hydroxyl and hydroperoxy radical uptake coefficients on water and sulfuric acid surfaces, J. Phys. Chem., 96, 4979–4985, 1992.

Hoffmann, M., and Calvert, J.: The aqueous phase chemistry, in: Chemical Transformation Modules for Eulerian Acid Deposition Models, National Center for Atmospheric Research Boulder, CO, 147–189, 1985.

Hoigné, J., and Bader, H.: Rate constants of reactions of ozone with organic and inorganic compounds in water—I: non–dissociating organic compounds, Water Res., 17, 173–183, 1983.

Huang, L. B., Zhao, Y., Li, H., and Chen, Z. M.: Kinetics of heterogeneous reaction of sulfur dioxide on authentic mineral dust: effects of relative humidity and hydrogen peroxide, Environ. Sci. Technol., 49, 10797–10805, 10.1021/acs.est.5b03930, 2015.

Huie, R. E., and Neta, P.: Rate constants for some oxidations of S (IV) by radicals in aqueous solutions, Atmos. Environ., 21, 1743–1747, 1987.

Jacob, D. J.: Chemistry of OH in remote clouds and its role in the production of formic acid and peroxymonosulfate, J. Geophys. Res. Atmos., 91, 9807–9826, 1986.

Kerr, J., and Calvert, J.: Chemical Transformation Modules for Eulerian Acid Decomposition Models, Volume I: The gas–phase chemistry, Boulder, Colorado, 1984.

Kukui, A., Borissenko, D., Laverdet, G., and Le Bras, G.: Gas–phase reactions of OH radicals with dimethyl sulfoxide and methane sulfinic acid using turbulent flow reactor and chemical ionization mass spectrometry, J. Phys. Chem. A, 107, 5732–5742, 2003.

Lee, Y.–N.: Atmospheric aqueous–phase reactions of nitrogen species, Brookhaven National Lab., Upton, NY (USA), 1984.

Liang, J. Y., and Jacobson, M. Z.: A study of sulfur dioxide oxidation pathways over a range of liquid water contents, pH values, and temperatures, J. Geophys. Res. Atmos., 104, 13749–13769, doi:10.1029/1999jd900097, 1999.

Lin, C., Rohatgi, N., and DeMore, W.: Ultraviolet absorption cross sections of hydrogen peroxide, Geophys. Res. Lett., 5, 113–115, 1978.

Lind, J. A., and Kok, G. L.: Henry's law determinations for aqueous solutions of hydrogen peroxide, methylhydroperoxide, and peroxyacetic acid, J. Geophys. Res. Atmos., 91, 7889–7895, 1986.

Martin, L., Easton, M., Foster, J., and Hill, M.: Oxidation of hydroxymethanesulfonic acid by Fenton's reagent, Atmos. Environ., 23, 563–568, 1989.

Maruthamuthu, P., and Neta, P.: Phosphate radicals. Spectra, acid–base equilibriums, and reactions with inorganic compounds, J. Phys. Chem., 82, 710–713, 1978.

McElroy, W.: An Experimental Study of the Reactions of Some Salts of Oxy–sulphur Acids and Reduced Sulphur Compounds with Strong Oxidants (O_3, H_2O_2 and HSO_5), Central Electricity Generating Board (CEGB) Technology Planning and Research Division, 1987.

Mellouki, A., Jourdain, J., and Le Bras, G.: Discharge flow study of the CH_3S+ NO_2 reaction mechanism using Cl+ CH_3SH as the CH_3S source, Chem. Phys. Lett., 148, 231–236, 1988.

Michel, A. E., Usher, C. R., and Grassian, V. H.: Reactive uptake of ozone on mineral oxides and mineral dusts, Atmos Environ, 37, 3201–3211, 10.1016/S1352–2310(03)00319–4, 2003.

Molina, L. T., and Molina, M. J.: UV absorption cross sections of HO_2NO_2 vapor, J. Photochem., 15, 97–108, 1981.

Munger, J. W., Tiller, C., and Hoffmann, M. R.: Identification of hydroxymethanesulfonate in fog water, Science, 231, 247–250, 1986.

Nicovich, J., and Wine, P.: Temperature ‐ dependent absorption cross sections for hydrogen peroxide vapor, J. Geophys. Res. Atmos., 93, 2417–2421, 1988.

Nip, W., Singleton, D., and Cvetanovic, R.: Gas–phase reactions of O (^{3}P) atoms with methanethiol, ethanethiol, methyl sulfide, and dimethyl disulfide. 1. Rate constants and Arrhenius parameters, J. Am. Chem. Soc., 103, 3526–3530, 1981.

O'Sullivan, D. W., Lee, M., Noone, B. C., and Heikes, B. G.: Henry's law constant determinations for hydrogen peroxide, methyl hydroperoxide, hydroxymethyl hydroperoxide, ethyl hydroperoxide, and peroxyacetic acid, J. Phys. Chem., 100, 3241–3247, 1996.

Olson, T. M., and Hoffmann, M. R.: Hydroxyalkylsulfonate formation: its role as a S (IV) reservoir in atmospheric water droplets, Atmos. Environ., 23, 985–997, 1989.

Rettich, T. R.: Some photochemical reactions of aqueous nitrous acid, Diss. Abstr. Int. B, 38, 5968, 1978.

Sander, S. P., Friedl, R., Golden, D., Kurylo, M., Moortgat, G., Wine, P., Ravishankara, A., Kolb, C., Molina, M., and Finlayson–Pitts, B.: Chemical kinetics and photochemical data for use in atmospheric studies evaluation number 15, 2006.

Schwartz, S., and White, W.: Solubility equilibria of the nitrogen oxides and oxyacids in dilute aqueous solution, Adv. Environ. Sci. Eng.;(United States), 4, 1981.

Schwartz, S. E.: Gas–Phase and Aqueous–Phase Chemistry of HO_2 in Liquid Water Clouds, J. Geophys. Res. Atmos., 89, 1589–1598, doi:10.1029/JD089iD07p11589, 1984.

Sehested, K., Rasmussen, O. L., and Fricke, H.: Rate constants of OH with HO_2, O_2^-, and $H_2O_2^+$ from hydrogen peroxide formation in pulse–irradiated oxygenated water, J. Phys. Chem., 72, 626–631, 1968.

Sehested, K., Holcman, J., and Hart, E. J.: Rate constants and products of the reactions of e–aq, dioxide (1-)(O_2^-) and proton with ozone in aqueous solutions, J. Phys. Chem., 87, 1951–1954, 1983.

Sillen, L. G., Martell, A. E., and Bjerrum, J.: Stability constants of metal–ion complexes, Chemical Society London, 1964.

Staehelin, J., and Hoigne, J.: Decomposition of ozone in water: rate of initiation by hydroxide ions and hydrogen peroxide, Environ. Sci. Technol., 16, 676–681, 1982.

Strehlow, H., and Wagner, I.: Flash photolysis in aqueous nitrite solutions, Zeitschrift für Physikalische Chemie, 132, 151–160, 1982.

Thomas, J.: The rate constants for H atom reactions in aqueous solutions, J. Phys. Chem., 67, 2593–2595, 1963.

Treinin, A., and Hayon, E.: Absorption spectra and reaction kinetics of NO_2, N_2O_3, and N_2O_4 in aqueous solution, J. Am. Chem. Soc., 92, 5821–5828, 1970.

Tyndall, G., and Ravishankara, A.: Kinetics of the reaction of the methylthio radical with ozone at 298 K, J. Phys. Chem., 93, 4707–4710, 1989.

Underwood, G. M., Song, C. H., Phadnis, M., Carmichael, G. R., and Grassian, V. H.: Heterogeneous reactions of NO_2 and HNO_3 on oxides and mineral dust: A combined laboratory and modeling study, J. Geophys. Res. Atmos., 106, 18055–18066, doi:10.1029/2000jd900552, 2001.

Vaghjiani, G. L., and Ravishankara, A.: Absorption cross sections of CH_3OOH, H_2O_2, and D_2O_2 vapors between 210 and 365 nm at 297 K, J. Geophys. Res. Atmos., 94, 3487–3492, 1989.

Wagner, C., Schuster, G., and Crowley, J.: An aerosol flow tube study of the interaction of N_2O_5 with calcite, Arizona dust and quartz, Atmos. Environ., 43, 5001–5008, 2009.

Wexler, A. S., and Clegg, S. L.: Atmospheric aerosol models for systems including the ions H^+, NH_4^+, Na^+, SO_4^{2-}, NO_3^-, Cl^-, Br^-, and H_2O, J. Geophys. Res. Atmos., 107, 2002.

Wine, P., Tang, Y., Thorn, R., Wells, J., and Davis, D.: Kinetics of aqueous phase reactions of the SO_4^- radical with potential importance in cloud chemistry, J. Geophys. Res. Atmos., 94, 1085–1094, 1989.

Yin, F., Grosjean, D., and Seinfeld, J. H.: Photooxidation of dimethyl sulfide and dimethyl disulfide. I: Mechanism development, J. Atmos. Chem., 11, 309–364, 1990.

Zhou, X., and Mopper, K.: Apparent partition coefficients of 15 carbonyl compounds between air and seawater and between air and freshwater; implications for air–sea exchange, Environ. Sci. Technol., 24, 1864–1869, 1990.